Hindawi
Advances in Materials Science and Engineering
Volume 2021, Article ID 6672746, 9 pages
https://doi.org/10.1155/2021/6672746

Research Article

Fabrication of Tantalum and Hafnium Carbide Fibers via Forcespinning™ for Ultrahigh-Temperature Applications

Harold O. Lee,[1] Patricia H. Caraballa,[2] Avi G. Bregman,[1] Nelson S. Bell,[1] James R. Nicholas,[1] Marissa Ringgold,[1] and LaRico J. Treadwell[1]

[1]*Sandia National Laboratories, Advanced Materials Laboratory, Albuquerque 87106, NM, USA*
[2]*University of New Mexico, Albuquerque 87106, NM, USA*

Correspondence should be addressed to LaRico J. Treadwell; ljtread@sandia.gov

Received 17 December 2020; Revised 1 April 2021; Accepted 12 April 2021; Published 26 April 2021

Academic Editor: Patrice Berthod

In this work, a novel method for producing ultrafine tantalum and hafnium carbide fibers using the Forcespinning™ technique via a nonhalide-based sol-gel process was investigated. An optimal solution viscosity range was systematically determined via rheological studies of neat PAN/DMF as a function of fiber formation. Subsequently, Forcespinning™ parameters were also systemically studied to determine the optimal rotational velocity and spinneret-to-collecting rod distance required for ideal fiber formation. TaC and HfC fibers were synthesized via Forcespinning™ utilizing a mixture of PAN and refractory transition metal alkoxides (i.e., tantalum (V) ethoxide and hafnium (IV) tert-butoxide) in DMF solution based on optimal conditions determined from the neat PAN/DMF. In all instances after calcination, powder X-ray diffraction (PXRD) and energy dispersive spectroscopy (EDS) indicated that TaC and HfC fibers were produced. TGA/DSC confirmed the chemical stability of the resulting fibers.

1. Introduction

While refractory transition metal-carbides (RTM-Cs) have been studied as far back as the 1800s, interest in these materials increased in the late 1950s as the space race intensified [1]. Research of RTM-Cs gained even more interest during the late 1980s for aerospace applications [1]. As hypersonic technology pushes speeds beyond Mach 5, surface temperatures can reach upwards to 2000°C in the presence of highly reactive gas species [1]. Therefore, materials that can survive/mitigate these extreme environments are critical for the future application of hypersonic technologies. Currently, carbon/carbon (C/C) composites are the material of choice due to their mechanical, thermal, and shock properties. Unfortunately, carbon is susceptible to oxidation at high temperature in various environments and has poor stability in strong erosion environments [2]. Silicon carbide (SiC) fibers have also been investigated as a replacement for carbon fibers. However, SiC fibers can only retain their mechanical properties up to 1900°C. SiC generates gaseous reaction products through native oxidation from a combination of >1100°C, high pressure, and external gas flow [3]. Due to the thermal limitation of carbon and silicon carbide fibers handicapping ultrahigh-temperature performance, RTM-C materials for use in high-temperature environments have been identified as viable replacements [4]. RTM-C materials possess strong covalent bonding and degrees of metallic bonding that lead to high melting points (>3700°C (4000 K)), high hardness, good high-temperature strength, high resistance to oxidation, excellent electrical conductivity, and exceptional resistance to harsh chemical and thermal environments [2, 5–7]. This combination of properties allows RTM-Cs to survive in more extreme environments than that of existing structural materials. Therefore, utilizing these materials as fiber reinforcements in composites would significantly enhance the thermal resistance as well as the damage tolerance in ultrahigh-temperature composites [2–7].

To use these RTM-C materials as fiber reinforcements in composites, a readily scalable route to produce high quality materials in fiber form is critical. Methods to produce hafnium and tantalum carbide (HfC and TaC) materials

from literature have reported several routes that have led to the successful production of these materials in fiber and powder form [8]. However, most of these methods utilize harsh reagents and halide precursors of the refractory transition metal, which are known to lead to impurities upon degradation (i.e., Cl-contamination). The sol-gel process has demonstrated the feasibility to utilize metal alkoxides (groups IV, V, and VI) to synthesize particles and fibers, with little to no impurities [9–12].

Furthermore, these methods are not all conducive to produce quality fibers through traditional techniques. Currently, the most common ways to fabricate fibers include melt-spinning, self-assembly, phase separation, and electrospinning methods [13]. Due to the simplicity and low-cost operation of electrospinning, it is the most commonly used method to fabricate nanofibers. Unfortunately, this technique has material/solvent limitations due to electrostatic fields and intrinsically low throughput via traditional lab scale electrospinning fabrication which has shown only to produce around 0.1 g/h of fibers [14, 15]. On the other hand, Oregon et al. produced polycaprolactone (PCL) fibers at a rate of 0.32 g in two minutes (scaled up to 9.6 g/h) via the Forcespinning™ technique which corresponds to a 3000% increase in output [14]. Forcespinning™ is a process developed by Sarker et al. that is similar to electrospinning. However, it uses centrifugal forces instead of electrostatic forces to generate fibers from a solution ejected from a spinning metal head [15]. This leads to the rapid production of fibrous materials ranging from nanoscale to micron scale [16]. By using centrifugal forces, the viable material options for Forcespinning™ are not limited by their dielectric properties allowing a wide spectrum of material combinations [17–20]. By combining Forcespinning™ with the sol-gel process, ultrahigh-temperature ceramic fibers such as silicon carbide (SiC) and RTM-C fibers such as titanium carbide (TiC) and zirconium carbide (ZrC) have been previously synthesized successfully. While Firbas et al. were the first to produce TiC and ZrC fibers via the Forcespinning™ technique, higher melting point TaC and HfC have yet to be synthesized via this method [17].

In this work, a method for producing stable TaC and HfC fibers using the Forcespinning™ technique and nonhalide-based sol-gel metal precursors is introduced. First, an ideal solution viscosity was systematically determined via rheological studies of neat PAN/DMF. Next, Forcespinning™ parameters were systemically studied to determine the optimal angular velocity and spinneret-to-collecting rod distance required for ideal fiber formation. Lastly, sol-gel preparation, fiber processing parameters, and characterization data were presented for TaC and HfC fibers. To our knowledge, this is the first time TaC and HfC fibers have been synthesized via Forcespinning™. With these results, the high-throughput production of RTM-C fibers for reinforcements in composites is now viable through the Forcespinning™ technique.

2. Materials and Methods

2.1. Materials. All syntheses were performed inside an argon-filled glovebox, and all chemicals were used as received unless otherwise noted. Anhydrous dimethylformamide (DMF), anhydrous acetic acid, polyacrylonitrile (PAN, MW 150,000), and tantalum (V) ethoxide were purchased from Sigma Aldrich. Hafnium (IV) tert-butoxide was purchased from Alfa Aesar.

2.2. PAN Solution Preparation. PAN solutions were prepared at various weight percentages ranging from 10 to 20% w/w. To prepare solutions, desired amounts of PAN and DMF were added to a chemical jar with a magnetic stir bar. The solution was then sealed and allowed to stir until PAN was completely dissolved. A 3 mL aliquot of the PAN solution was drawn for the spinning process, and 1 mL aliquot was drawn for rheological studies to compare the various PAN solution weight percentages.

2.3. RTM-C Precursor Solution Preparation. Fiber precursor solution consisted of a PAN solution and tantalum (V) ethoxide solution combined. The PAN solution (13% w/w) recipe consisted of 3.897 g of PAN and 30.00 g of DMF. The reactants were added to a chemical jar with a magnetic stir bar; the solution was sealed and allowed to stir until PAN was completely dissolved. For the tantalum (V) ethoxide solution, 4.500 g of tantalum (V) ethoxide and 9.000 g of acetic acid was added to a chemical jar with a magnetic stir bar; the solution was sealed and allowed to stir until dissolved. The "fiber solution" was tantalum (V) ethoxide/acetic acid solution mixed with the PAN/DMF solution, which was stirred overnight. Lastly, a 3 mL aliquot of the fiber solution was drawn for the spinning process, and 1 mL aliquot was drawn for rheological studies to compare to the optimal neat PAN solution. The same process was used with hafnium (IV) tert-butoxide, instead of tantalum (V) ethoxide to generate HfC-fibers.

2.4. RTM-C Fiber Preparation. The fibers were generated using the FibeRio L-1000 M Cyclone Forcespinning™ System. The Forcespinning™ technique uses centrifugal force to extrude the solution out of metal heads onto vertical metal rods at chosen radial separation distances. Spin speed and collecting rod distance were systematically studied, and results are seen in the manuscript and supporting information. Systematic studies led to the ideal program being a multistep program consisting of spinning at 1000 rpm for the five seconds and then ramping up to 3500 rpm for 1200 seconds. The metal rods were placed 17.78 cm away from the spinneret. The resulting fibers were then collected and placed in a box furnace at 220°C with a ramp rate of 5°C per minute and then were held at 220°C for two hours. After cooling to room temperature, the fibers were then placed in a tube furnace at 1600°C with 5°C per minute ramp rate under the flow of argon and dwelled for two hours. The resulting fibers were characterized by PXRD, SEM/EDS, and TGA.

2.5. Fiber Characterization. Powder X-ray diffraction (PXRD) patterns were collected on a PANalytical X'Pert Pro diffractometer (5–70° two theta) employing CuKα radiation

(1.5406 Å) and a RTMS X'Celerator detector at a scan rate of 0.02°/sec using a zero-background holder. The PXRD patterns were analysed using JADE 9.6.0 software (Materials Data Inc., Livermore, CA) and indexed using the Powder Diffraction File PDF-4+. Thermogravimetric analyses (TGA)/differential scanning calorimetry (DSC) analyses were taken under flowing air and nitrogen atmosphere from room temperature to 1000°C at a ramp rate of 10°C/min using a Mettler Toledo STARe System. Scanning electron microscopy was conducted using a Hitachi S-5200 FE-SEM with an Oxford Instruments X-MAX EDAX accessory operating with an accelerating voltage of 20 kV.

3. Results and Discussion

3.1. Rheological Testing. The production of fiber materials is nontrivial and relies on numerous synthetic and instrumental variables. Of the many parameters, the viscosity of the sol-gel is the most readily and easily tailorable to produce fiber materials in any instrument. Therefore, rheological studies were done on PAN/DMF solutions to determine the optimal solution viscosity needed to produce fibers via Forcespinning™ utilizing our instrumentation.

Rheological testing of the neat PAN/DMF solutions of various weight percentages from 10 to 20 wt% was measured as a function of shear rate. Forcespinning™ polymer solutions are generally higher in polymer content than electrospinning solutions, due to the variation in the jet generation and extension behavior of the two methods. The neat solution served as a surrogate to identify the optimal conditions for RTM-C solutions, and their viscosity profile results are shown in Figure 1(a). At 10 wt % (lowest loading), the PAN/DMF solution displays nearly Newtonian behavior, up to a shear rate of ~200 1/s, with a viscosity of 570 mPa s.

As PAN content is increased, the polymer solutions show increasing viscosity levels, and the transition to shear thinning behavior occurs at progressively lower shear rates, as the system shows further chain entanglement. All these solutions are expected to have chain entangled character, based on prior literature of PAN/DMF solutions [20]. The stable formation of a fiber requires a polymer concentration sufficient to obtain chain entanglement. Wang et al. presented rheological characterization of PAN/DMF solutions that determined a minimum concentration ($C_{\min}$) for the entry into the chain entanglement regime at approximately 5 wt%. For polymer solutions above $C_{\min}$, Wang et al. found that the specific viscosity follows the power law $\eta_{sp} \sim \phi^{4.78}$ [21]. Figure 1(b) plots the specific viscosity vs. volume % PAN for estimation of the power law characteristic for these solutions. The higher concentration solutions made here differ in molecular weight and have a power law exponent of 6.25, indicating rapid development of elastic character with drying.

The production of fibers involves the surface tension and viscosity of the polymer solution, chain entanglement and relaxation dynamics of the polymer solution, evaporation rate of the solvent, and extension forces on the fiber in transit from the orifice tip to the collector system [22]. Fiber production by Forcespinning™ was first tested on pure PAN/DMF solutions to correlate solutions viscosity with fiber formation, as viscoelastic instabilities can lead to formation of beads when viscosity is low. As can be seen from Figure 2, the average viscosity obtained from a shear rate ranging from 0 to 1000 1/s of the different solutions increased as the PAN wt % increased. The 10–13 wt % solution yielded poor nanofiber morphology with droplets and beads due to low viscosity as seen in Figure S2. The 17–20 wt % produced short nanofibers of low yield indicating that the viscosity of the solution is too high for the given centrifugal force as seen in Figure S2. However, the 15 wt % yielded uniform fibers with no droplets. The measured viscosity in Figure 1(a) is shear thinning, and therefore, values at the highest shear rate of 1000 1/s were chosen to characterize suitable fiber production. This gives 2.80 Pa s as the viscosity target for the RTM-C precursor solution.

Control over fiber properties including diameter, regularity, and shape requires tailoring the processing parameters of the Forcespinning™ process. Operationally, there are three instrument parameters which can be varied to control fiber formation: angular velocity, Ω, collector distance, and the polymer concentration. Forcespinning™ has a five-step process of fiber formation. The steps include (1) jet exit, (2) orbital trajectory, (3) aerodynamic fiber vibration, (4) orbital expansion, and (5) fiber collection. There is a critical angular velocity to produce a jet, but there is a second critical angular velocity in which the jet diameter is reduced well below the tip orifice diameter [8]. Thus, the fiber size is relatively insensitive to the orifice diameter, which is important for the capillary backpressure needed to induce flow to the tip. There is a minimum rotational speed related to the fiber extension phase as well to prevent the fibers from being pulled back to the spinneret shaft, and a maximum speed related to the break-up of the polymer solution jet. Therefore, the 15 wt % PAN solution was investigated at different speeds and collector distances to determine the optimal conditions. As seen in Figure S3, fiber formation is drastically affected by varying spin speeds and collecting distances. Low rpms (≤2000 rpm) lead to droplet formation due to not exceeding the second critical angular velocity needed to reduce the fiber diameter below the orifice diameter. Too high (≥5000 rpm) of spin speed leads to very small fibers that lack enough strength to form continuous fibers. The collecting distance also needs to be optimized in order to determine at which distance from the spinneret the fibers are fully formed. Therefore, we investigated distances ranging from around 15 cm–18 cm for the collector. Systematic investigation of these variables based on the fiber formation and yield led to 3500 rpm and a collecting distance of 17.78 cm to be the optimal speed and distance required for the best fiber formation.

It was anticipated that the addition of the tantalum (V) ethoxide/acetic acid solution to the 15% wt PAN/DMF solution would increase the viscosity, ultimately leading to a change of solution performance under the previously determined conditions. From previous studies with pure PAN/DMF solution, the optimal solution viscosity required for our instrumentation was 2.80 Pa s. To account for the additional attraction between Ta-ethoxide and PAN, we

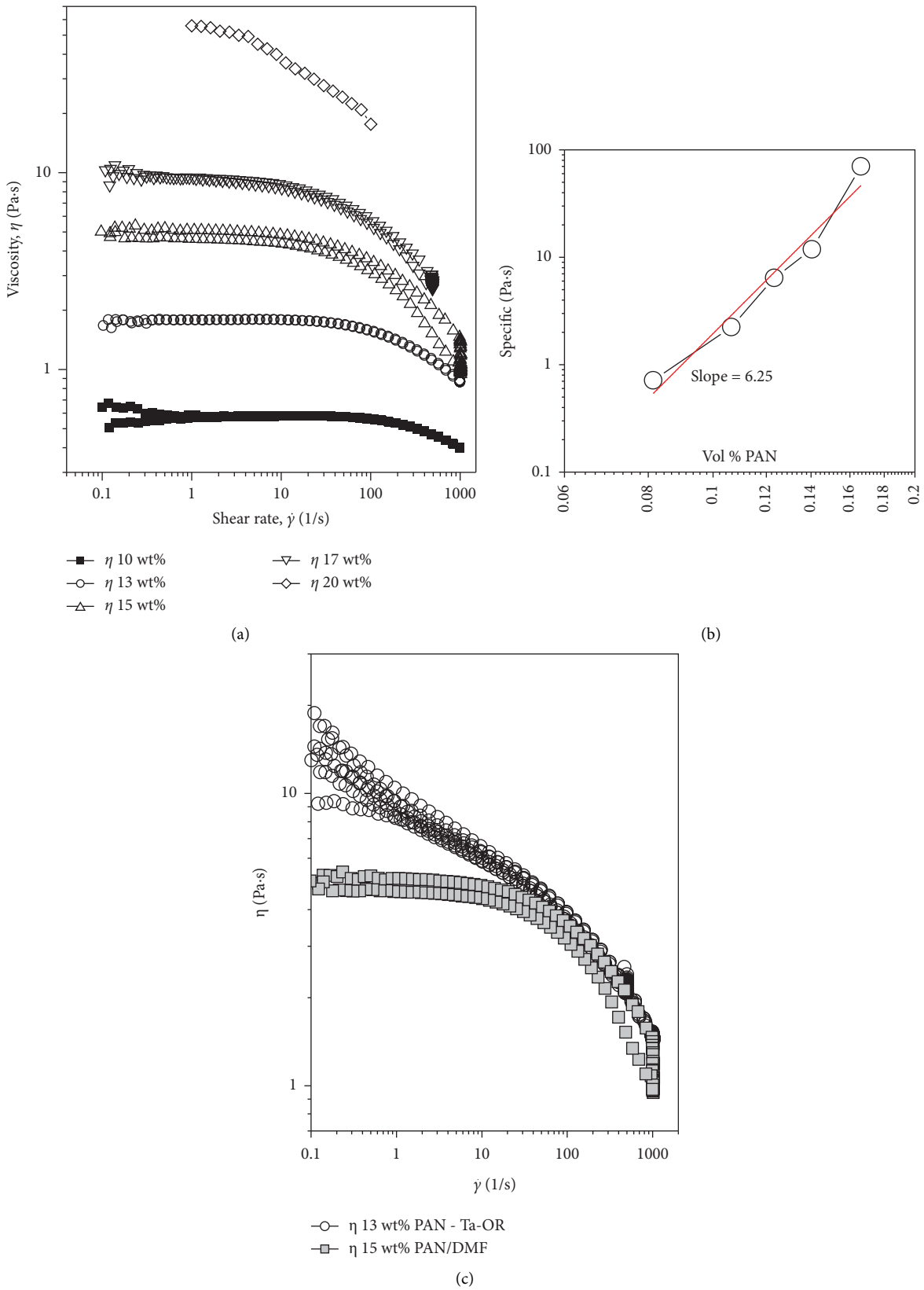

Figure 1: (a) Viscosity versus shear rate of w/w PAN/DMF solution as a function of PAN content. (b) Specific viscosity vs. vol % PAN solution. (c) Comparison of 15 wt % PAN solution to 13 wt % PAN-Ta-OR precursor solution, showing similar high shear rate flow properties.

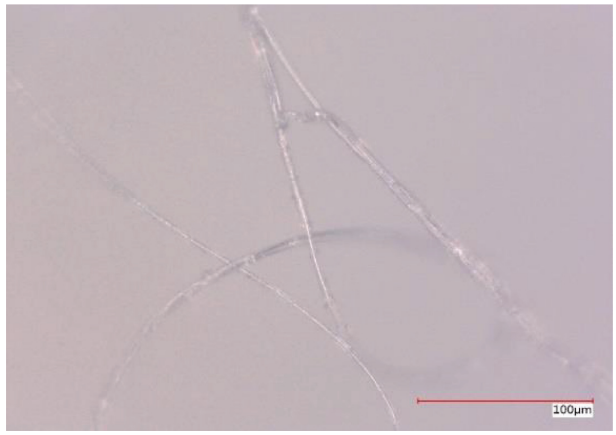

Figure 2: Image of fiber formed from 15% w/w PAN/DMF solution when spun at 3500 rpm and collecting rods at 17.78 cm away from the spinneret.

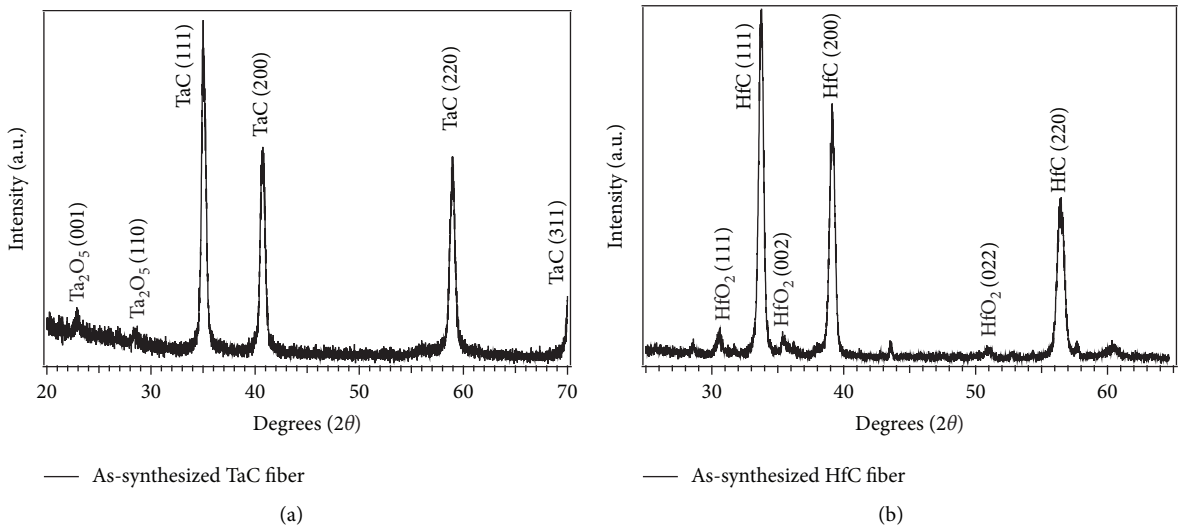

Figure 3: (a) PXRD spectra of as-synthesized TaC indexed with TaC (PDF# 00-035-0801). (b) PXRD spectra of as-synthesized HfC indexed with HfC (PDF# 00-039-1491).

reduced the PAN/DMF concentration to 13 wt % resulting in a total of 33 wt % tantalum (V) ethoxide/acetic acid solution to generate the "fiber solution." The rheology of the fiber solution was investigated, in comparison with the neat 15 wt % PAN/DMF solution, and their behavior was comparable as seen in Figure 1(c). At low shear rate, the viscosity for the TaC precursor fiber solution is higher than the 15 % PAN/DMF solution, indicating that the Ta-ethoxide generates additional interaction between the PAN chains. The 1000 1/s shear rate viscosity of the TaC precursor was 3.07 Pa s, which is comparable to the 15% PAN/DMF solution determined to be optimal. This procedure was replicated for the Hf tert-butoxide/acetic acid solution. Thus, these solutions were used throughout the rest of this work. After the RTM-C fiber solution was made, the fiber materials were generated at 3500 RPM with the collecting rods at 17.78 cm away from the spinneret.

3.2. PXRD. After green body curing at 220°C and carbonization at 1600°C of the reagents, PXRD data were collected on the isolated products. As seen in Figure 3(a), the product from the Ta "fiber solution" yielded diffraction peaks at 35.5° (111), 40.7° (200), 58.9° (220), and 70.0° (311) which was indexed to TaC (PDF #00-035-0801) [6, 21–26]. There was some presence of tantalum oxide (Ta_2O_5, PDF #00-025-0922) as this is typical when using metal alkoxides as a metal precursor [11]. Using semiquantitative (S-Q) phase analysis in Bruker's Diffrac Eva V5.2 software, it was estimated that Ta-fibers were 91.8% TaC (00-035-0801) and 8.2% Ta_2O_5 (00-025-0922).

Figure 3(b) presents the PXRD spectra of the product obtained from the Hf solution. The spectra exhibited diffraction peaks at 33.4° (111), 38.8° (200), and 56.1° (220) which was indexed to HfC (PDF #00-039-1491). Remnants of hafnium oxide (HfO_2, PDF #00-053-0560) are present as

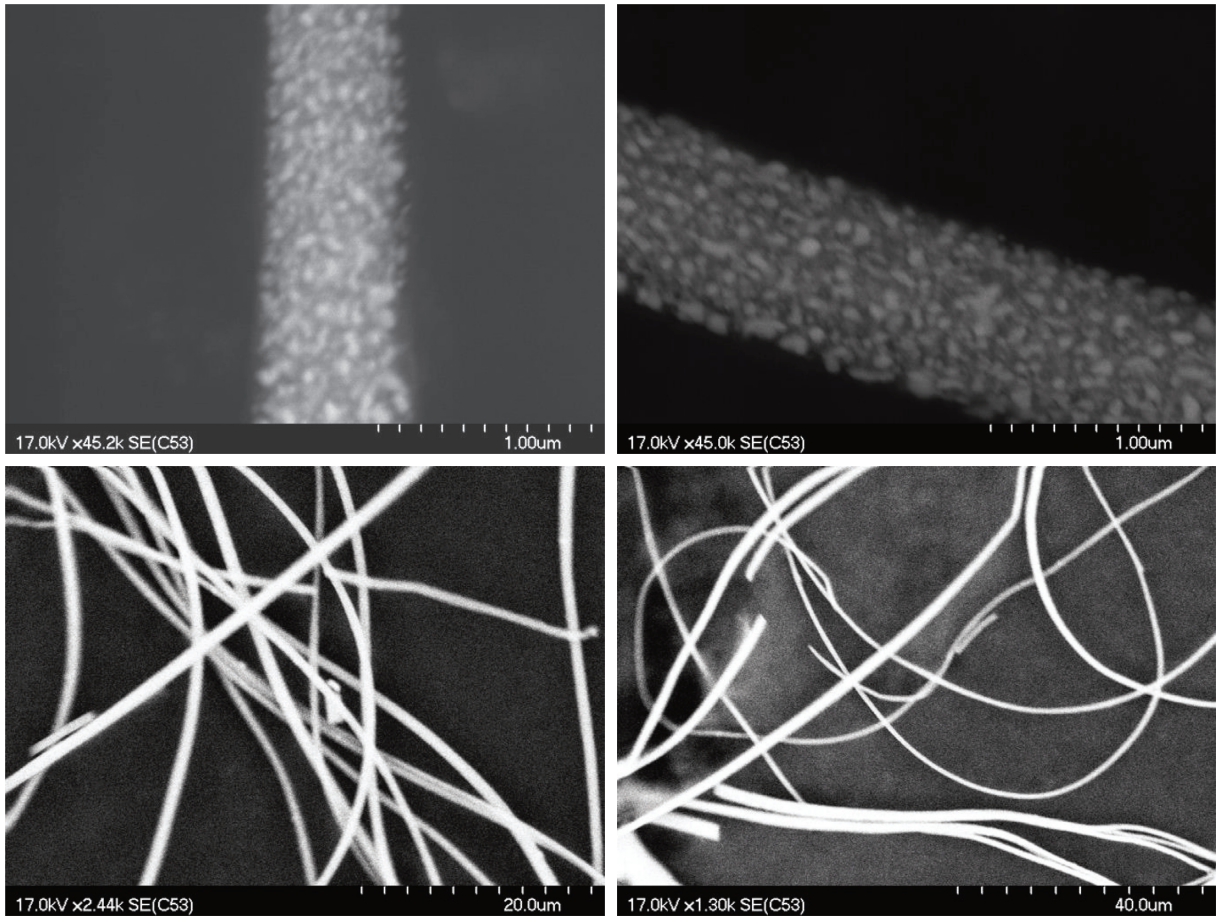

Figure 4: SEM images of as-spun TaC fibers after carbonization.

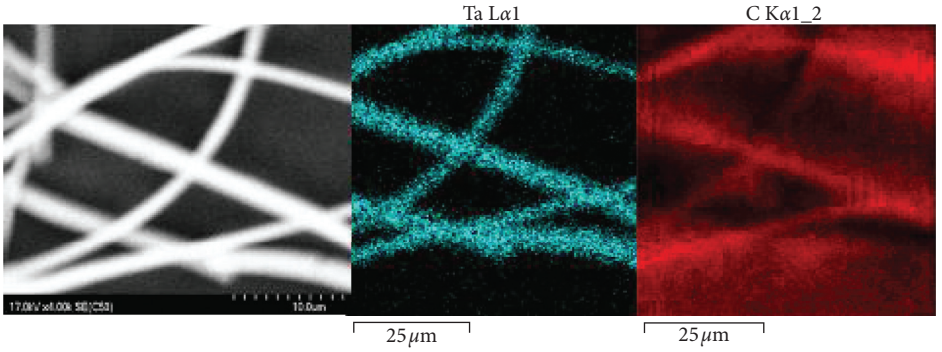

Figure 5: EDS analysis of as-spun TaC fibers after carbonization.

seen in the spectra as this is typical when using metal alkoxides as a metal precursor, but the major product is HfC [11]. Using semiquantitative (S-Q) phase analysis in Bruker's Diffrac Eva V5.2, it was estimated that Hf-fibers were 96.8% HfC (00-039-1491) and 3.2% HfO_2 (00-053-0560).

3.3. SEM/EDS. Figure 4 shows the SEM images of the as-synthesized TaC fibers. The TaC fibers exhibited diameters with an average size of 475 nm. Figure 5 presents the SEM image along with EDS images of tantalum and carbon collected on the TaC fibers. The EDS analysis confirms the presence of tantalum and carbon over the selected area as seen in the bottom image. Figure 6 shows the SEM images of the as-synthesized HfC fibers. The HfC fibers exhibited diameters with an average size of 340 nm. Figure 7 presents the SEM image along with EDS images of hafnium and carbon collected on the HfC fibers. The EDS analysis confirms the presence of hafnium and carbon over the selected area as seen in the bottom image.

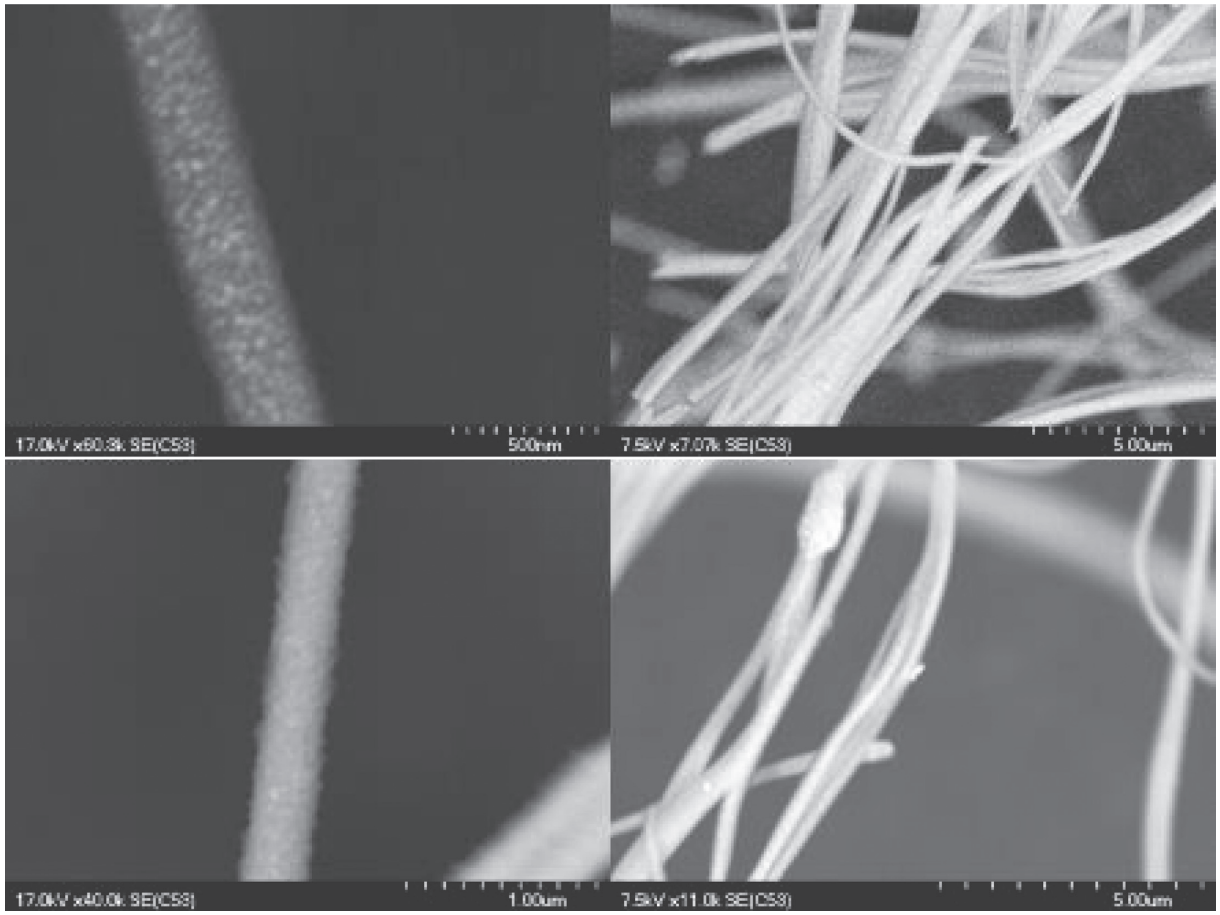

Figure 6: SEM images of as-spun HfC fibers after carbonization.

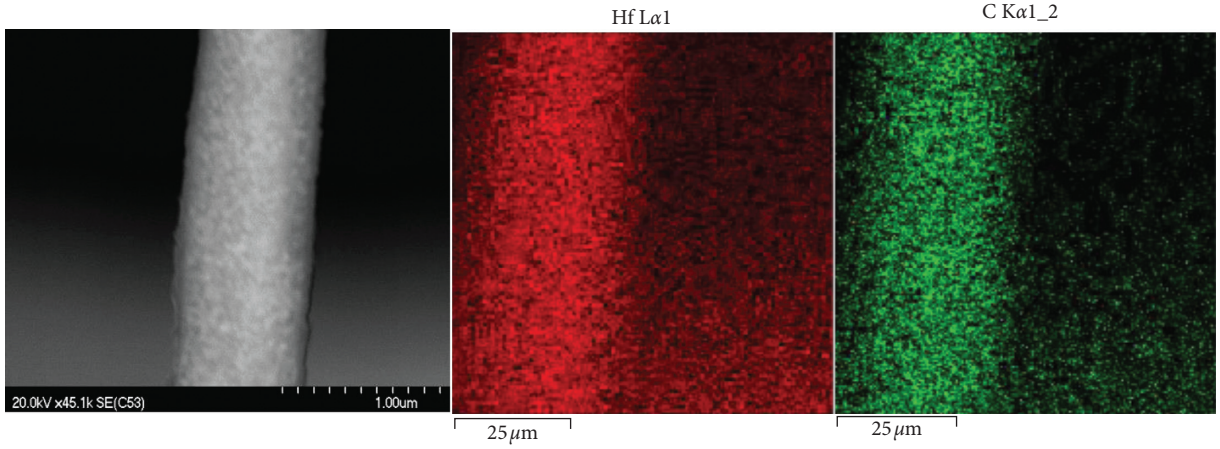

Figure 7: EDS analysis of as-spun HfC fibers after carbonization.

3.4. Thermal Behavior of RTM-C Fibers. The TGA curve in Figure 8(a) shows that the TaC fibers were thermally stable below around 450°C while in air. After 450°C, an increase in weight was observed which is attributed to the oxidation of TaC to Ta_2O_5 which is further verified by PXRD as seen in S4 [6, 22]. Note that the magnitude of this weight increase indicates that oxidation may be limited to the surface of TaC via the formation of a Ta_2O_5 passivation layer being formed. The oxidation mechanism of TaC is as follows [27] [29]:

$$4TaC + 9O_2 \longrightarrow 2Ta_2O_5 + 4CO_2 \quad (1)$$

After around 560°C, the weight loss was due to the oxidation of any free carbon present and loss of CO_2 from the system [20]. Also, as seen in Figure 8(b), the fibers

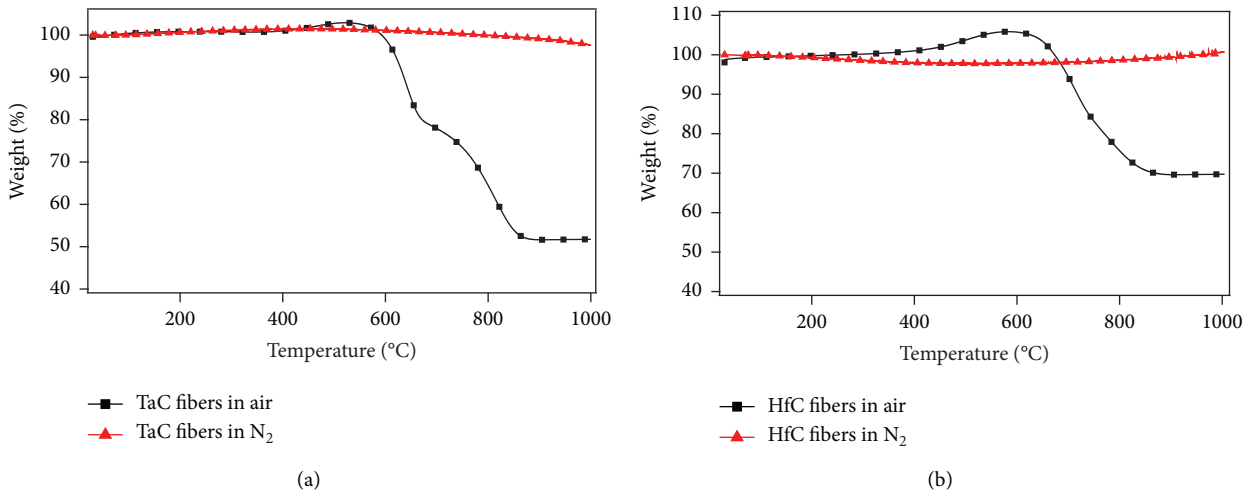

Figure 8: (a) TGA curve of TaC fibers in air and in inert environment (N_2). (b) TGA curve of HfC fibers in air and in inert environment (N_2).

exhibited no change in mass (decomposition) under N_2. The TGA curve in Figure 8 shows that the synthesized HfC fibers exhibited thermal stability below around 500°C while in air.

After 500°C, an increase in mass was observed due to the oxidation of HfC to HfO_2 and verified by PXRD (S4). The oxidation of HfC is as follows [21, 22]:

$$HfC + 2O_2 \longrightarrow HfO_2 + CO_2 \quad (2)$$

After around 650°C, the weight loss was due to the oxidation of any free carbon present and loss of CO_2 from the system [20]. Also, as seen in Figure 8(b), the fibers exhibited no change in mass (decomposition) under N_2. Note that the weight increases at around 500°C is larger, and the weight decreases at around 650°C which is smaller than that of the TaC fibers. This may be due to the possibility that TaC fibers had more trapped free carbon than the HfC fibers. Raman spectra are presented in Figure S4.

4. Conclusions

TaC and HfC fibers have been successfully synthesized via the Forcespinning™ method. The rheology of the varying wt % of PAN and DMF was determined to understand the entanglement and optimize the precursor solution for fiber formation. This surrogate sample solution led to the optimal fiber solution parameters to produce RTM-C fibers. The RTM-C fibers were characterized in order to confirm their formation, crystal structure, and stability. Upon successful heat treatment of the fiber, PXRD confirmed the formation of crystalline TaC and HfC fibers. TGA analysis showed that the RTM-C fibers maintain oxidation resistance and thermal stability in air up to 450°C. Microscopy analysis determined the average diameter of the fibers was 475 nm and 340 nm for TaC and HfC fibers, respectively. Also, microscopy showed that Hf and Ta were distributed evenly throughout the fiber. This method allows for simple and rapid synthesis of these fibers with the ability to make grams of fibers quickly. Ongoing studies will examine the mechanical behavior, decreasing oxide content, and fiber incorporation in the composite.

Data Availability

The rheological, powder X-ray diffraction, scanning electron microscopy/energy dispersive spectroscopy, and thermogravimetric analysis data used to support the findings of this study are included within the article.

Conflicts of Interest

The authors declare no conflicts of interest.

Acknowledgments

This work was supported by the Laboratory Directed Research and Development program at Sandia National Laboratories, a multimission laboratory managed and operated by National Technology and Engineering Solutions of Sandia LLC, a wholly owned subsidiary of Honeywell International Inc., for the U.S. Department of Energy's National Nuclear Security Administration under contract DE-NA0003525.

Supplementary Materials

The supplementary information includes detailed pictures of PAN fiber formation at various speeds and collecting rod distances, PXRD spectra of fibers after thermogravimetric analysis in air, and Raman spectra of as-synthesized fibers. (*Supplementary Materials*)

References

[1] W. G. Fahrenholtz and G. E. Hilmas, "Ultra-high temperature ceramics: materials for extreme environments," *Scripta Materialia*, vol. 129, pp. 94–99, 2017.

[2] A. Vinci, L. Zoli, D. Sciti, J. Watts, G. E. Hilmas, and W. G. Fahrenholtz, "Mechanical behaviour of carbon fibre reinforced TaC/SiC and ZrC/SiC composites up to 2100°C," *Journal of the European Ceramic Society*, vol. 39, no. 4, pp. 780–787, 2019.

[3] W. G. Fahrenholtz, G. E. Hilmas, I. G. Talmy, and J. A. Zaykoski, "Refractory diborides of zirconium and hafnium," *Journal of the American Ceramic Society*, vol. 90, no. 5, pp. 1347–1364, 2007.

[4] Q. J. Hong and A. Van De Walle, "Prediction of the material with highest known melting point from ab initio molecular dynamics calculations," *Physical Review B*, vol. 92, no. 2, pp. 1–6, 2015.

[5] K. A. Khalil, E. S. M. Sherif, A. M. Nabawy, H. S. Abdo, W. W. Marzouk, and H. F. Alharbi, "Titanium carbide nanofibers-reinforced aluminum compacts, a new strategy to enhance mechanical properties," *Materials (Basel)*, vol. 9, no. 5, pp. 1–14, 2016.

[6] R. D. Vispute, S. Hullavarad, A. Luykx et al., "Epitaxy and recrystallization kinetics of TaC thin films on SiC for high temperature processing of semiconductor devices," *Applied Physics Letters*, vol. 90, no. 24, pp. 3–5, 2007.

[7] J. Ma, Y. Du, M. Wu, and M. Pan, "One simple synthesis route to nanocrystalline tantalum carbide via the reaction of tantalum pentachloride and sodium carbonate with metallic magnesium," *Materials Letters*, vol. 61, no. 17, pp. 3658–3661, 2007.

[8] M. Jalaly, F. J. Gotor, and M. J. Sayagués, "Mechanochemical combustion synthesis of vanadium carbide (VC), niobium carbide (NbC) and tantalum carbide (TaC) nanoparticles," *International Journal of Refractory Metals and Hard Materials*, vol. 79, pp. 177–184, 2019.

[9] H. Preiss, D. Schultze, and E. Schierhorn, "Preparation of NbC, TaC and Mo2C fibres and films from polymeric precursors," *Journal of Materials Science*, vol. 33, no. 19, pp. 4687–4696, 1998.

[10] K. Nakane, N. Ogata, and Y. Kurokawa, "formation of inorganic (TaC, TaN) fibers by thermal decomposition of cellulose acetate-tantalum alkoxide precursor gel fibers," *Journal of Applied Polymer Science*, vol. 100, no. 6, pp. 4320–4324, 2006.

[11] E. P. Simonenko, N. A. Ignatov, N. P. Simonenko, Y. S. Ezhov, V. G. Sevastyanov, and N. T. Kuznetsov, "Synthesis of highly dispersed super-refractory tantalum-zirconium carbide Ta4ZrC5 and tantalum-hafnium carbide Ta4HfC5 via sol-gel technology," *Russian Journal of Inorganic Chemistry*, vol. 56, no. 11, pp. 1681–1687, 2011.

[12] J. Cheng, X. Wang, J. Wang, and H. Wang, "Synthesis of a novel single-source precursor for HfC ceramics and its feasibility for the preparation of Hf-based ceramic fibres," *Ceramics International*, vol. 44, no. 6, pp. 7305–7309, 2018.

[13] Z. M. Zhang, Y. S. Duan, Q. Xu, and B. Zhang, "A review on nanofiber fabrication with the effect of high-speed centrifugal force field," *Journal of Engineered Fibers and Fabrics*, vol. 14, 2019.

[14] V. A. Agubra, L. Zuniga, D. D. La Garza, L. Gallegos, M. Pokhrel, and M. Alcoutlabi, "Forcespinning: a new method for the mass production of Sn/C composite nanofiber anodes for lithium ion batteries," *Solid State Ionics*, vol. 286, pp. 72–82, 2016.

[15] A. Salinas, M. Lizcano, and K. Lozano, "Synthesis of β-SiC fine fibers by the forcespinning method with microwave irradiation," *Journal of Ceramics*, vol. 2015, pp. 1–5, 2015.

[16] P. Firbas, A. Seeber, and Y.-B. Cheng, "Creation of titanium and zirconium carbide fibers with the forcespinning technique," *International Journal of Applied Ceramic Technology*, vol. 13, no. 4, pp. 619–628, 2016.

[17] Z. Yang, H. Peng, W. Wang, and T. Liu, "Crystallization behavior of poly (ε-caprolactone)/layered double hydroxide nanocomposites," *Journal of Applied Polymer Science*, vol. 116, no. 5, pp. 2658–2667, 2010.

[18] N. Obregon, V. Agubra, M. Pokhrel et al., "Effect of polymer concentration, rotational speed, and solvent mixture on fiber formation using forcespinning," *Fibers*, vol. 4, no. 2, p. 20, 2016.

[19] K. Sarkar, C. Gomez, S. Zambrano et al., "Electrospinning to forcespinning," *Materials Today*, vol. 13, no. 11, pp. 12–14, 2010.

[20] C. Wang, H.-S. Chien, C.-H. Hsu, Y.-C. Wang, C.-T. Wang, and H.-A. Lu, "Electrospinning of polyacrylonitrile solutions at elevated temperatures," *Macromolecules*, vol. 40, no. 22, pp. 7973–7983, 2007.

[21] J. Diani, Y. Liu, and K. Gall, "Finite strain 3D thermoviscoelastic constitutive model for shape memory polymers," *Polymer Engineering and Science*, vol. 46, no. 4, pp. 486–492, 2006.

[22] S. Padron, A. Fuentes, D. Caruntu, and K. Lozano, "Experimental study of nanofiber production through forcespinning," *Journal of Applied Physics*, vol. 113, no. 2, 2013.

[23] S. Zhou, G. Zhou, S. Jiang, P. Fan, and H. Hou, "Flexible and refractory tantalum carbide-carbon electrospun nanofibers with high modulus and electric conductivity," *Materials Letters*, vol. 200, pp. 97–100, 2017.

[24] L. Feng, S.-H. Lee, and B.-L. Yoon, "Nano-TaC powder synthesized using modified spark plasma sintering apparatus and its densification," *Ceramics International*, vol. 41, no. 9, pp. 11637–11645, 2015.

[25] Z.-W. Cui, X.-K. Li, Y. Cong, Z.-J. Dong, G.-M. Yuan, and J. Zhang, "Synthesis of tantalum carbide from multiwall carbon nanotubes in a molten salt medium," *New Carbon Materials*, vol. 32, no. 3, pp. 205–212, 2017.

[26] M. Desmaison-Brut, N. Alexandre, and J. Desmaison, "Comparison of the oxidation behaviour of two dense hot isostatically pressed tantalum carbide (TaC and Ta2C) materials," *Journal of the European Ceramic Society*, vol. 17, no. 11, pp. 1325–1334, 1997.

[27] C. Zhang, A. Loganathan, B. Boesl, and A. Agarwal, "Thermal analysis of tantalum carbide-hafnium carbide solid solutions from room temperature to 1400°C," *Coatings*, vol. 7, no. 8, 2017.